5 November 1982, Volume 218, Number 4572 SCIENCE

# Fast Ion Bombardment of Ices and Its Astrophysical Implications

W. L. Brown, L. J. Lanzerotti, R. E. Johnson

*Summary.* Ices such as water, carbon dioxide, and methane are now known to be pervasive constituents of the solar system and probably of the interstellar medium as well. Many of these ices and ice-covered surfaces are exposed to bombardment by the energetic ions of space. Laboratory experiments have been carried out to study the effects of such bombardment. Surprisingly efficient erosion of ice layers is associated with electronic excitation of the ices by the ions. These results are a challenge to an understanding of the physical processes involved and have implications for a number of astrophysical problems of current interest.

Astronomical observations both from the earth and from spacecraft continue to expand the experimental evidence that ices are pervasive constituents of the solar system (*1*). Frozen volatiles are found in the polar caps of Earth and Mars, in the satellites of the giant planets (*2–4*), in the rings of Saturn (*4*), and in the nuclei of comets (*5*). The most prominent is water ice; carbon dioxide ice is definitely found on Mars (*6*), and Pluto and probably its companion moon are covered with methane frost (*7*). Volcanic Io has sulfur dioxide frost deposits (*8*). Particulate grains in the interplanetary medium can be ice or ice-covered (*9*). Indeed, except for the near proximity of individual stars, frozen volatiles may be the dominant surface constituents of interstellar grains and other solid, cold bodies throughout the galaxy.

Spacecraft measurements over the past two decades have shown that the solar system is filled with energetic ions. These ions are primarily hydrogen and helium with a wide range of energies and fluxes. Ions with energies of approximately 1 kilo electron volt per atomic mass unit comprise the solar wind, continually flowing out from the sun. Eruptions on the sun produce sporadic outbursts of solar cosmic rays with energies from tens of thousands to tens of millions of electron volts per atomic mass unit. Planets with magnetic fields, such as Earth, Jupiter, and Saturn, can trap such energetic ions in their radiation belts. Recognition that the ices are inevitably bombarded by at least some of these ions led to experiments (*10*) to measure the consequences of such bombardment in terms of the erosion and modification of ice layers and the formation of molecular fragments and more complex molecules.

It is well known that energetic ions incident on more conventional solids result in the ejection of atoms and molecules. The experiments conducted to date have produced a number of surprises. These have been a strong stimulus to efforts to understand the physical mechanisms involved when energetic ions interact with ices as well as the consequences of these interactions for some contemporary problems in astrophysics. In the following sections we discuss the experiments and our present understanding of the physical mechanisms and then address some applications to astrophysical problems.

## Laboratory Measurements

*Experimental conditions.* Studies of ion bombardment of ices were carried out with ice films condensed from the vapor on a cold metallic substrate. The inset in Fig. 1 illustrates the experimental arrangement. Films from a few hundred to a few thousand angstroms in thickness were grown at a typical rate of about 1000 Å per minute. Substrate temperatures were chosen to be well below the effective sublimation temperature for the ice being studied, for example, $< 160$ K for $H_2O$, $< 110$ K for $SO_2$, and $< 80$ K for $CO_2$. The base vacuum in the region of the substrate was less than $10^{-8}$ torr, maintained by a combination of turbomolecular and cryogenic pumping. The substrate was beryllium, which had been coated with a 50 Å gold layer to serve as a marker in measurements of film thickness.

The molecular thickness of the films after deposition and at successive stages of ion bombardment was monitored by Rutherford backscattering, usually with 1.5-MeV $He^+$ ions. Such scattering is due to the low but precisely known probability of an incident ion colliding with a nucleus in a nearly head-on collision. The energy of the backscattered ion depends on the mass of the nucleus with which it collided and the amount of material it traversed (losing energy) before and after the collision. The most sensitive measure of ice film thickness was provided by the energy of the backscattered helium ions from the gold marker layer under the ice. This gave a thickness sensitivity of ~ 10 Å. The backscattered helium ions also directly revealed heavy-atom constituents of a film, such as carbon, oxygen, and sulfur, giving an independent measure of the molecular thickness of the film and a measure of its stoichiometry at various stages of erosion (*11*).

Films were bombarded with hydrogen and helium ion beams (and in a few cases

W. L. Brown is head of the Radiation Physics Research Department and L. J. Lanzerotti is a member of the technical staff in the Electromagnetic Phenomena Research Department, Bell Laboratories, Murray Hill, New Jersey 07974. R. E. Johnson is a professor in the Department of Nuclear Engineering and Engineering Physics, University of Virginia, Charlottesville 22903.


0036-8075/82/1105-0525$01.00/0

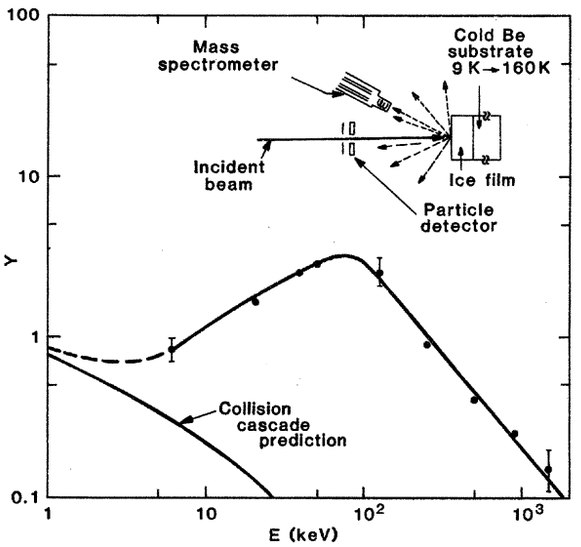


Fig. 1. Erosion yield as a function of the energy of hydrogen ions. (Inset) Schematic outline of experimental arrangement.

also with oxygen and carbon beams) with energies from ~ 10 keV to 2 MeV. Beams about 1 to 2 millimeters in diameter were defined by collimation. The erosion yield $Y$ (molecules lost per incident ion) was independent of beam current, and thus erosion occurred as a result of individual ions of the beam, not through macroscopic heating of the films by the total beam (*10*).

Quadrupole mass spectrometry was used to measure the molecular species ejected from the films during ion bombardment. It was also used in some cases to examine the fragments and new molecules formed in the films by ion bombardment and released from the films during subsequent thermal heating in the absence of ion bombardment (*12*).

*Experimental results*. Figure 1 shows the erosion yield of $H_2O$ ice bombarded with hydrogen ions (*11*). The erosion yield peaks at ~ 100 keV and falls rapidly at lower and higher energies. Also shown is a calculation of the expected loss of $H_2O$ from conventional ion sputtering, that is, sputtering due to the formation of collision cascades initiated in the ice by scattering of the incident ions from the nuclei of the ice atoms (*13*). Such a process is well understood and is known to be responsible for the loss of material in ion bombardment of metallic and semiconducting materials (*14*). The ices studied are all electronic insulators and it is clear that the material erosion from ices has a different origin.

The peak of $Y$ in Fig. 1 occurs at an energy close to the maximum in the electronic stopping power of protons in ice (*11*). The electronic stopping power of an incident ion, $(dE/dx)_e$, is the energy given up by the ion to ionization and excitation of the electrons of the material per unit path length of the ion. The data of Fig. 2 show clearly that electronic processes and not nuclear collisions control the erosion of the ice films. This is true for all of the ices we and others have examined: $H_2O$ (*10, 11, 15–18*), $CO_2$ (*17, 19*), $SO_2$ (*20*), $NH_3$ (*19*), $CH_4$ (*19*), Ne (*19*), Ar (*19, 21*), Kr (*19*), Xe (*18, 22*), $N_2$ (*23*), $H_2$ (*24*), and $O_2$ (*19*). Electronic processes have been found to lead to material erosion from other insulating solids, particularly the alkali halides (*25*) and also from less ionic insulators such as $UF_4$ (*26*), $LiNbO_3$ (*27*), and $Al_2O_3$ (*27*), although in the latter cases this is measurable only with ions having very high electronic stopping powers.

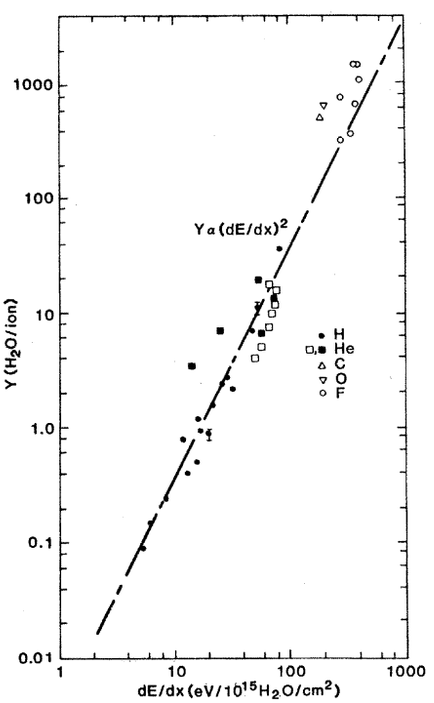


Fig. 2. Erosion yield for water ice at liquid nitrogen temperature as a function of $(dE/dx)_e$, the electronic energy loss of hydrogen, helium, oxygen, carbon, and fluorine ions. (●, ■, △, and ▽) data from (*11, 15*); (□) data from (*22*); (○) data from (*16*).

Figure 2 shows the dependence of $Y$ for $H_2O$ ice on the electronic stopping power of hydrogen, helium, and heavier ions (*10, 11*). It includes the data of Fig. 1, which are very well ordered to a single line by this plot. The dependence of $Y$ on $(dE/dx)_e$ is not linear, however. It varies approximately as $(dE/dx)_e^2$. A similar approximately quadratic dependence has been found at low temperature for all the ices that have been studied. The data for helium ions in Fig. 2 fall around the line defined by the hydrogen ions, with departures that are qualitatively understood (*28*). Figure 2 also contains two points for carbon and oxygen ions (*10*) at 1.5 MeV and a set of points obtained by Cooper and co-workers (*16*) with fluorine ions at energies up to 25 MeV. As for helium, there are systematic departures of the fluorine data from the hydrogen line, but the magnitude of $Y$ for this set of data is still in rough agreement with the quadratic dependence defined by the hydrogen results. However, the results for heavy ions suggest a steeper than quadratic dependence of erosion yield on $(dE/dx)_e$ at large stopping powers. This regime of high-energy heavy ions is rarely encountered in astrophysical situations, and thus we will focus on the region of lower $(dE/dx)_e$.

Figure 3 shows the temperature dependence of the erosion yield of $H_2O$ (*15–18*), $CO_2$ (*17, 19*), $SO_2$ (*17, 20*), and Ar (*21*) for million-electron-volt $He^+$ ions. The highest measurement temperature in each case is set by sublimation in the absence of ion bombardment. As experimental measurements typically require hundreds to thousands of seconds, a practical upper limit for the temperature corresponds to an equilibrium vapor pressure of ~ $10^{-7}$ torr, at which sublimation would result in a loss of ~ 0.1 monolayer per second. The material loss due to normal sublimation has been subtracted from the few data points for which it is significant. All the curves in Fig. 3 show a temperature-independent region at low temperatures. At higher temperatures, three different types of behavior are evident. Argon is the simplest, showing an abrupt increase in $Y$ at about 25 K. It has been suggested that this indicates a bombardment enhancement of normal sublimation a few degrees below the temperature at which sublimation alone limits the measurements (*21*). The $H_2O$ and $SO_2$ curves show a temperature-independent region at low temperatures with a continuous rise to the sublimation limit. For $CO_2$

there are two sharp steps upward in $Y$ at about 40 and 50 K. We associate the low-temperature region in all four cases with a direct ejection process (*17*), for which several possible models are discussed in the next section. The temperature dependence for $H_2O$, $CO_2$, and $SO_2$ we associate with diffusion of or reaction between molecular fragments formed in the ice films as a result of intramolecular bond breaking due to the ionization produced by the incident ions (*15, 17*). In the case of $H_2O$ ice, the major constituents involved in the high-temperature increase of $Y$ are $H_2O$ and $O_2$ molecules, the products of radiolysis in the ice (*29*).

The formation of new molecules from the bombardment of mixed ices has also been observed. One interesting case is that of a mixed ice of $H_2O$ and $CO_2$, deposited from a 50:50 molecular mixture of the two gases. To identify new species that might be produced and to reduce the background in the quadrupole mass spectrometer, $D_2{}^{16}O$ and $^{13}C^{18}O_2$ were used. New molecules were observed when the mixed ice layer, bombarded at 9 K, was subsequently heated to temperatures at which sublimation of $D_2O$ occurred relatively rapidly (*12*). Figure 4a shows the results in this case. Several masses were monitored during this experiment but only mass 33, corresponding to isotopically labeled formaldehyde, $D_2{}^{13}C^{16}O$, is represented in Fig. 4a. The sublimation peaks of mass 20 ($^2D_2{}^{16}O$) and mass 48 ($^{12}C^{18}O_2$) observed in the warm-up of a mixture of $^2D_2{}^{16}O$ and $^{12}C^{18}O_2$ without bombardment are shown in Fig. 4b. In Fig. 4b the sharp sublimation peak of $CO_2$ at the low-temperature edge of the $D_2O$ peak indicates that the $CO_2$ is held in the $H_2O$ ice; a $CO_2$ film alone would rapidly sublimate at ~ 80 K. The peak of mass 33 in Fig. 4a indicates that formaldehyde, formed by bombardment, behaves similarly (*12*).

The net production of formaldehyde (integral of curve 1 in Fig. 4a) is ~ 5 molecules per incident 1.5-MeV helium ion. The total number of ionization events for a $He^+$ ion passing through the ~ 1000 Å film is ~ 100. Thus the probability of formation of a formaldehyde molecule, instead of simple recombination of the ion pairs to reform the original molecules, is quite high. We also measured formaldehyde of mass 35, $^2D_2{}^{13}C^{18}O$, which was less abundant by a factor of about 3 than mass 33. This indicates that the fragmentation of both $D_2O$ and $CO_2$ molecules, required to produce mass 35, is less favorable than the reaction of a C ion, produced from $CO_2$ by the beam, with $D_2O$ to form $D_2CO$.

## Models of the Erosion Process

*Temperature-dependent erosion.* The temperature-dependent part of the erosion of ice films seems to be associated with radiation chemistry in the ices; ionization by a passing ion breaks bonds in the molecular solid and thus provides the opportunity for new bonds to form (*29*). At very low temperatures the new molecules may be unable to escape from the ice and hence unable to contribute to erosion of the ice layer. If the radiation is carried out at higher temperatures the molecules have higher diffusivities and are more likely to react and escape from the film (*19*). The gradual increases in erosion yield with temperature for $SO_2$ and $H_2O$ (Fig. 3) involve activation energies between 0.06 and 0.3 eV. In $H_2O$, these activation energies are comparable with those for free radicals that play an important role in radiation biology. However, the products leaving the film are not radicals, suggesting that secondary reactions take place. The steps in the yield curve for $CO_2$ (Fig. 3) suggest that two distinct new molecules are formed with low activation energies for diffusion ($\simeq$ 0.01 eV), perhaps CO and $O_2$. Further, after irradiation of $CO_2$ at a low temperature, as the sample is slowly heated without further radiation, there is additional material loss. This suggests that the exiting molecules are stored in the $CO_2$ at a low temperature and become mobile and escape as the temperature is raised.

These results and ideas only sketch the broad outlines of the temperature-dependent erosion process. There is obviously a great deal of detail missing; both more experiments and a more quantitative theory are needed.

*Temperature-independent erosion.* The temperature independence of the erosion yields at low temperatures indicates that the erosion process is not simple radiolysis. Direct release or ejection of molecules or atoms occurs from a large number of ices, including the rare gas atomic solids. A major question is how the electronic ionization and excitation energy deposited by the incident ion is converted into kinetic energy of motion of the molecules or atoms. In a metal or semiconductor the electronic energy spreads rapidly laterally from the incident particle track, by electron motion in the metal or by electron-hole diffusion in a semiconductor. By the time it is converted to motion of the nuclei (for instance, heat), the energy density is too low to supply the sublimation energy needed to eject a molecule from the surface. The low mobility of positive charge (*28*) in insulating solids effectively prevents diffusion of the electronic excitation away from the close vicinity of the track. This localization of the ion cloud is a distinguishing feature of ice films. In addition, the ionization energy of an insulator is much larger than that of a metal or semiconductor. The energy is thus stored in relatively large units within the localized region, particularly when

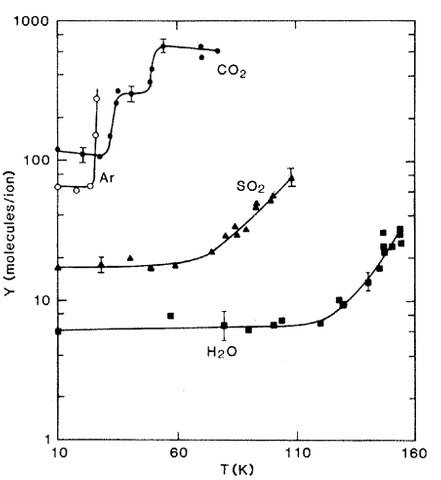


Fig. 3 (left). Temperature dependence of $Y$ for $H_2O$, $SO_2$, $CO_2$, and Ar ices for helium ions. The argon points (*21*) were taken for 0.75-MeV $He^+$; the other ices were eroded by 1.5-MeV $He^+$. The curves are drawn to guide the eye.

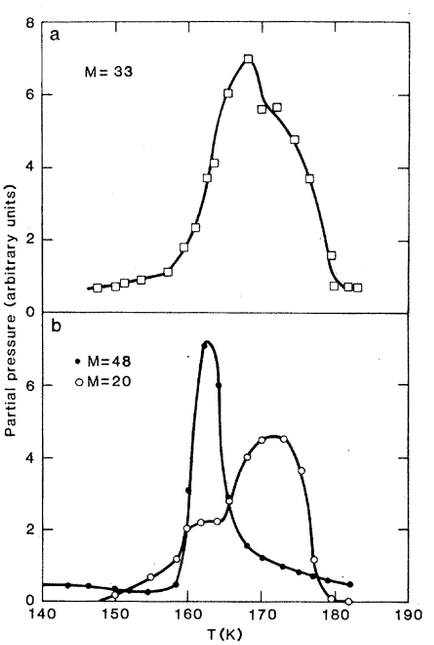


Fig. 4 (right). Quadrupole spectrometer measurements of the evolution of several molecules during warm-up of a mixed film of $CO_2$ and $H_2O$. The curves are drawn to connect the data points. (a) Evolution of mass 33 formaldehyde from a $^{13}C^{18}O_2$-$D_2{}^{16}O$ ice film following irradiation at 9 K with 1.5-MeV $He^+$ ions. (b) Evolution of mass 48, $^{12}C^{18}O_2$, and mass 20, $D_2{}^{16}O$, from $^{12}C^{18}O_2$-$D_2{}^{16}O$ ice film without radiation.

compared with the relatively small intermolecular binding energy of molecular ices.

In general, there are two ways to convert electronic energy to kinetic energy of motion of lattice atoms and molecules: (i) collisions between the free electrons and lattice atoms or ions (electron-phonon interactions) and (ii) Coulomb repulsion between insufficiently screened nuclei. The latter may be exemplified by excitation of repulsive molecular states within a molecule (*28, 30*) [the analog of dissociative recombination in the gas phase (*31*)] or direct repulsion between neighboring molecular ions (*28*), or an ion and the electric field of a collection of other ions (*11, 28, 32*). Two models that attempt to account for the experimental results in the temperature-independent regime are discussed below.

*Thermal spike*. In this model all or part of the electronic energy deposited by a passing ion is considered to be converted rapidly and locally to heat. A transiently hot cylinder of material is thus associated with each ion track (*11, 18, 22, 26, 33*). Where this cylinder intersects the surface in a hot disk, sublimation can occur, as indicated schematically in Fig. 5a. The hot cylinder grows larger in radius and lower in temperature with time due to radial thermal conduction. For this picture to give erosion yields as large as those measured, the electronic-to-thermal energy transfer must occur in $< 10^{-11}$ second. If it is slower, radial diffusion of the heat produced will never allow the disk to be hot enough to sublimate significantly. Such a model is appealing because, for an initially narrow cylindrical spike, it predicts an erosion yield that depends on $(dE/dx)_e^2$ (*11, 33*), as found experimentally for light ions.

There are two major difficulties with this model. The first is the time for the energy transfer. Fast conversion of about 20 percent of the electronic energy loss would be sufficient to account for the erosion yield observed for several different ices (*28*). It may be that such a fraction is available through a fast nonradiative recombination process involving repulsive molecular states (*30*). Alternatively, it may be provided through free electrons scattering with lattice atoms or ions (*34*). Nevertheless, rapid energy transfer by such processes remains highly speculative. The second difficulty is the spatial distribution of the electronic energy increments converted to heat. They must be close together in a line to justify the cylindrical approximation that leads to a $(dE/dx)_e^2$ dependence. For million-electron-volt $H^+$ ions the spacing between individual ionization events along the track is probably too large to satisfy this requirement.

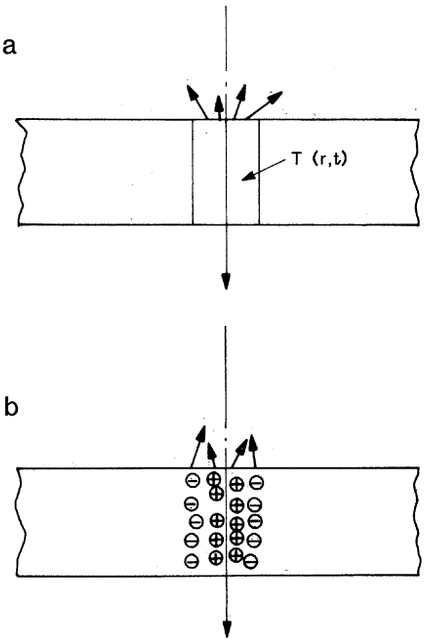


Fig. 5. Schematic models of the temperature-independent erosion process: (a) thermal spike; (b) Coulomb ejection.

*Coulomb repulsion*. This model focuses on the macroscopic radial distribution of charge immediately following the passage of an ion. In the ionization cascade initiated by the incident ion, electrons are kinetically displaced away from the ion's path and create, at least momentarily, a separated charge distribution consisting of a shell of electrons surrounding a core of positive ions, as shown schematically in Fig. 5b (*35*). For high $(dE/dx)_e$, the energy in the space charge electric field may be a significant fraction of the total energy given up by the incident ion (*28*).

The sign of the electric field is such as to accelerate the positive ions outward, as discussed by Fleischer *et al.* (*35*) in connection with the formation of damage tracks in insulating minerals by high $(dE/dx)_e$ particles. The process has been called a Coulomb explosion. At the surface of an insulating film, there are axially outward components of the electric field that may produce ejection of particles from the surface. Such a model also has a $(dE/dx)_e^2$ dependence (*11, 32*), essentially because the electric field energy density is proportional to the square of the charge density.

This model also has problems. The first is the time duration of the separated charge distribution. If the electrons that were displaced outward are not immobilized by being rapidly and deeply trapped at their extended radial positions (as they are, for instance, in polar liquids), they will return to neutralize the positive charge before the heavy positive ions can be set in motion. However, if the free electrons are very mobile and do return due to the Coulomb field, the potential energy that existed in the separated charge configuration will be converted to kinetic energy of the electrons (*28*). The electrons will then oscillate back and forth through the positive ion cloud until they lose their energy to lattice vibrations (heat) (*34*). During this time, there will still be a net negative charge outside the positive ion core, tending to accelerate the positive ions both radially and toward the surface. Whether this is sufficient to provide the observed erosion is uncertain.

The low $(dE/dx)_e$ regime in this model, as well as in the thermal spike model, results in a loss of cylindrical symmetry. In this limit for the Coulomb repulsion case, the probability of ejection can be considered in terms of one ionized center acting repulsively on an adjacent center. The $(dE/dx)_e$ dependence in this limit remains quadratic because it involves the statistics of two ionization events, one close to the surface and the second close to the first (*28*). Again, it is difficult to make quantitative calculations based on this model, although the values of the parameters required to explain the experimental results do not seem unreasonable (*11*).

Seiberling *et al.* (*26*) proposed that at high $(dE/dx)_e$, Coulomb repulsion may be a way of rapidly converting electronic energy to heat. Since this conversion depends on $(dE/dx)_e^2$ and the thermal spike sublimation yield depends on the square of the heat input, this model appears to lead to a yield varying as $(dE/dx)_e^4$. Such a model has been suggested as one way of accounting for the high values of erosion yield of $H_2O$ ice with million-electron-volt carbon, oxygen, and fluorine ions (Fig. 2) and the erosion yield of $UF_4$ (*26*) and other room-temperature insulating solids (*27*).

The models above are discussed in more detail by Johnson and Brown (*28*). At this stage, the details of the decay of the electronically excited track and the transfer of enough kinetic energy to molecules to cause their ejection from a solid surface are not clear. Measurements of the velocity distribution of the ejected condensed gas species and extension of the measurements to ejection by incident electrons should help to clarify the decay and erosion process.

## Implications and Applications in Astrophysics

The gravitational attraction of a body is a major factor determining the net loss of ejected material due to ion bombardment of its surface. Atoms and molecules will be ejected from a surface with a distribution in energy that depends on the physical mechanisms of the erosion process. [For collision cascade sputtering of metals this distribution is well characterized (*14, 36*); it is essentially unknown for electronically induced erosion of a condensed gas.] If the energy required for gravitational escape from a body is much larger than the mean ejection energy, then sputtering will predominantly redistribute material across the surface, and the escape fraction will be determined by the tail of the energy distribution. For small icy objects with negligible gravitational attraction, such as comets (a few kilometers in diameter), planetary ring particles (centimeters to meters), and ice grains (tens to thousands of micrometers), most of the sputtered material will be lost to space. The relevant parameters for several astrophysical bodies of interest are given in Table 1.

Table 1. Escape energies and velocities from the surfaces of various solar system bodies.

| Object | Radius (km) | Density ($g/cm^3$) | $g$ ($cm/sec^2$) | Escape energy (eV/amu) | Escape velocity (m/sec) |
|---|---|---|---|---|---|
| Jovian satellites | | | | | |
| Io | 1,820 | 3.5 | 178 | 0.035 | 2,580 |
| Europa | 1,500 | 3.5 | 147 | 0.023 | 2,080 |
| Ganymede | 2,640 | 2.0 | 147 | 0.040 | 2,790 |
| Callisto | 2,500 | 1.6 | 114 | 0.029 | 2,390 |
| Saturnian satellites | | | | | |
| Mimas | 195 | 1.2 | 6.6 | 0.00013 | 150 |
| Enceladus | 250 | 1 | 7 | 0.0002 | 190 |
| Tethys | 525 | 1.1 | 15 | 0.0008 | 400 |
| Dione | 560 | 1.4 | 22 | 0.0013 | 500 |
| Rhea | 765 | 1.3 | 28 | 0.0023 | 660 |
| Titan | 2,570 | 1.9 | 136 | 0.0036 | 2,640 |
| A-ring object | $\sim$ 0.001 | $\sim$ 1 | $\sim 2.6 \times 10^{-5}$ | $\sim 2.6 \times 10^{-15}$ | $\sim 7.2 \times 10^{-4}$ |
| Moon | 1,738 | 3.34 | 164 | 0.029 | 2,400 |
| Earth | 6,378 | 5.5 | 980 | 0.64 | 11,200 |

On a planetary satellite, in addition to the gravitational effect, the incident radiation must reach the surface in order to be an altering influence. If a body has an intrinsic magnetic field, or is immersed in the field of another body, the trajectory of incident ions will be altered so as to exclude bombardment of some regions of the surface for ions lower than a certain energy. Areas of preferential particle bombardment (*37*) can also result from the interaction of the planetary magnetic fields with the intrinsic field or surface conductivity of a moon. This appears to occur with the Jovian satellite Io. Electrons and ions flowing along Jupiter's magnetic field lines are directed into the polar regions of the moon (*38*).

An atmosphere around a satellite will prevent particles with energies lower than a certain value from reaching any part of the surface. In fact, charged particles can produce a self-limiting atmosphere (*39*): the erosion of surface ices by such ions can build up an atmosphere that will ultimately prevent the lower energy particles from striking the surface. A balance will result between exclusion of the low-energy particles and erosion of the surface by the higher energy particles at a sufficient rate to maintain an atmospheric equilibrium (*40*).

A molecule or atom eroded from the surface of a moon by a charged particle can suffer a variety of fates, as illustrated in Fig. 6. It can escape directly or can strike the surface again (Fig. 6a), depending on the gravitational attraction of the body and the sputtered particle energy. If a body has sufficient atmosphere, the outgoing sputtered particle will collide with atmospheric constituents, lose energy, and ultimately be absorbed on the surface (Fig. 6b). A particle eroded from a body can be ionized by solar or stellar photons or by an external plasma (Fig. 6c). Such ionized species can escape from the body, especially if there is an externally imposed magnetic field (such as a planetary or interplanetary magnetic field). In the case of Jupiter, for example, the planetary rotation speed, and hence the rotation speed of the planetary magnetic field, at the orbital locations of the large Galilean satellites (Table 1) is greater than the orbital speeds of the moons (*41*). Ionized species that find themselves on the planetary field lines are thus quickly swept away from the moon (*42*).

*Large bodies*. On the Galilean moons, erosion of ices by charged particles will result primarily in redistribution of the ice on the surfaces. In contrast, on the moons of Saturn, which have much lower gravitational escape velocities (Table 1), the eroded species will escape into the planet's magnetosphere (*43*). On the earth's moon, the redistribution of any frozen volatiles by sputtering by the solar wind and magnetosphere particles (due to electronically induced erosion processes) would effectively eliminate the possibility of surface water ice in the polar regions of that body (*44*). However, as illustrated in Fig. 6c, even eroded species in ballistic, bound trajectories or in an atmosphere can be lost from a satellite if the time for their ionization by

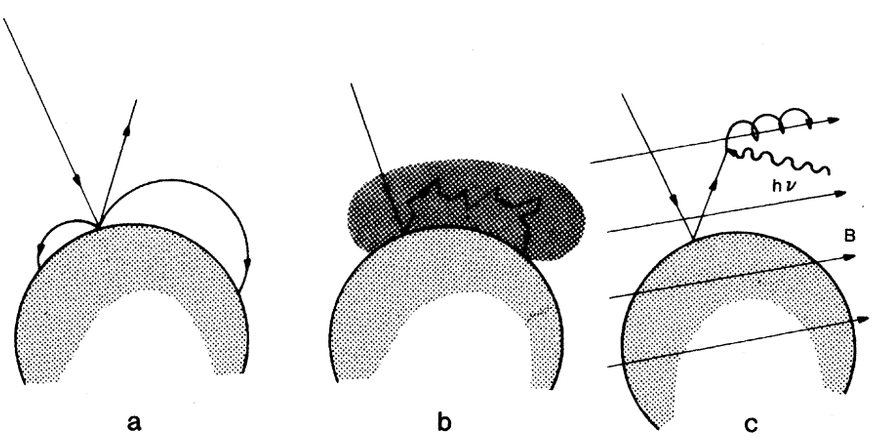


Fig. 6. Schematic illustration of possible fates of material eroded from a surface, depending on the gravitational attraction and external environment of the object. (a) An eroded atom or molecule can escape or enter into a ballistic trajectory, depending on its ejection energy and the gravitational attraction of the object; (b) an atmosphere can cause scattering and reimpact of the ejected species on the surface; or (c) ionization by solar photons ($h\nu$) of an ejected species in the presence of an externally imposed magnetic field can cause a loss of the species. In practice, various combinations of these three conditions can also exist.

solar radiation (photons) or by magnetospheric particles is short compared to the time between their ejection and their return to the surface.

Results of calculations of the redistribution of ice across the surface of a satellite after sputtering by energetic ions are shown in Fig. 7 (*43*). The distribution of incident ions was taken to have an anisotropy characteristic of those observed in the vicinity of the Galilean satellites (*45*). (An isotropic incident ion flux would, of course, not produce any net redistribution of material.) The curves in Fig. 7 are labeled by the ratio of the effective temperature (expressed as an energy) of the ejected particle velocity distribution (assumed to be Maxwellian) to the satellite escape energy. The loss or gain of material is measured with respect to the "original" surface. When the energy ratio is sufficiently large, a significant amount of material is lost to space at all latitudes; for a small ratio, the primary effect is redistribution, with surface thickness increasing at higher latitudes. The net difference in the erosion effect between equatorial and polar regions is dependent on the anisotropy of the incident ion flux. Such a redistribution effect might contribute, for example, to the occurrence of polar frost on Ganymede above about 40° in latitude. Using preliminary velocity distributions and measured erosion yields, the net growth of the surface would only be of the order of 1 meter over an eon ($10^9$ years), but still could account for the maintenance of an observed frost estimated to be a few millimeters thick (*46*).

Sputtered water molecules could form the basis for a tenuous atmosphere around some of the Galilean moons (*39, 40, 47, 48*), particularly if the surface ices have temperatures low compared to the full-body albedo temperatures of the moon (*49*). Calculations based on particle fluxes measured by Voyager 1 (which produce erosion by both collision cascade and electronic processes) indicate that an atmospheric column density on Ganymede could be as a high as $\sim 10^{14}$ $H_2O$ molecules per square centimeter, which is consistent with upper limits established by ultraviolet measurements by the Voyager spacecraft (*3*). Decomposition of ice by energetic ions, indicated by the production of $O_2$ in sputtering experiments at the higher temperatures (*17*), could lead to a larger column density on a satellite with a significant ice coverage. The $O_2$ produced would not condense on a surface with a temperature $\gtrsim 100$ K; such $O_2$ would only be lost by ionization or dissociation (*48*).

Similarly, the sputtering (by both the cold and hot magnetospheric plasmas) of $SO_2$ frost deposits on Io, in the polar regions and in colder regions away from active volcanoes, could form tenuous, localized $SO_2$ atmospheres with densities $\lesssim 10^{17}$ cm$^{-2}$ (*20*). Even before laboratory data were available, sputtering was considered to play a role in providing material from Io to the Jovian magnetosphere (*42*). The sputtered particles are probably gravitationally bound, so their loss would occur through ionization by the Jovian plasma or solar photons and then sweeping up by the Jovian magnetic field (see Fig. 6c). Such swept-up ions may be important in establishing the composition and density of the Jovian magnetospheric plasma, which is known to have significant levels of sulfur and oxygen ions (*50*).

*Small bodies*. The spectacular A and B rings of Saturn are the best known manifestations of small ice particles in the solar system (*4*). Measurements by the low energy charged particle instrument on Voyager showed that the Saturnian magnetospheric particle fluxes decreased strongly in intensity in the vicinity of the faint E ring and the moons Dione and Tethys (*51*). If the particle losses measured by Voyager were primarily due to collisions with the moons and the E ring (rather than, for example, wave-particle interactions), then the sputtering of ices from these objects could be a local source (*52*) of the heavy-ion plasma observed by a Pioneer 11 experiment (*53*) and a determinate of the lifetime of the E ring ($\sim 10^5$ years for 10-μm particles without replenishment). On the other hand, sputtering of ice particles on the A ring by energetic ions in Saturn's magnetosphere does not appear to play a role in producing the hydrogen atmosphere found around the ring (*52, 54, 55*), as originally proposed (*56*).

Icy bodies in interplanetary space in the solar system—for example, grains, comets, and the recently discovered minor planet Chiron—can be eroded by solar flare particles and the solar wind (electronic erosion process). The erosion rate ($\Delta r$ per year) is shown in Fig. 8 as a function of radial distance from the sun for water ice eroded by the solar wind (taken to be 10 protons per cubic centimeter at 1 astronomical unit with an energy of $\sim$ 1 keV) and one "typical" solar particle event per year (with a flux of about $10^{11} >$ 100-keV particles per square centimeter) (*19, 57*). Although the average helium-to-hydrogen ratio in solar flares is only $\sim$ 0.03 (*58*), the erosion from solar flare helium ions is comparable to the effect of the more abundant hydrogen ions because of the much larger $dE/dx$ of the helium ions.

Particle erosion effects dominate the mass loss process for 20-μm grains in the

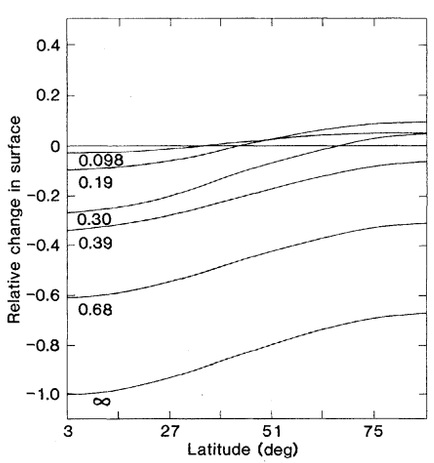


Fig. 7 (left). Relative change in surface height as a function of latitude for water ice erosion by an ion flux with anisotropy typical of that measured in the vicinity of the Galilean satellites in the Jovian magnetosphere. Fig. 8 (right). Erosion rate of surfaces of $H_2O$ and $CO_2$ ices as a function of distance from the sun for the solar wind and one typical solar flare event per year. Also shown are the sublimation rates. The dotted enhancements on the $CO_2$ curves are meant to schematically illustrate enhanced erosion at that distance because of release of fragments formed by irradiation at colder temperatures (greater distances).

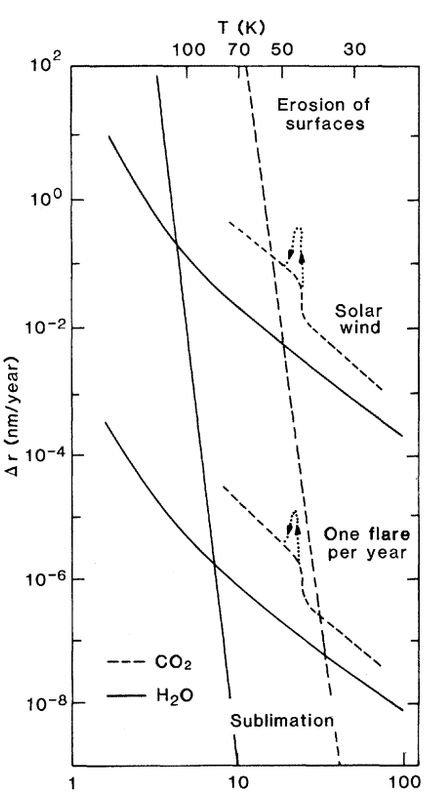

inner solar system (*57, 59, 60*) and for objects of all sizes beyond about 7 AU (*19*). However, even over an eon, the loss from solar wind sputtering is insignificant at large distances—for example, ~ 1 mm at 30 AU (about the distance of Neptune and the aphelion of Halley's comet) for a water ice body. This thickness loss could increase by a factor of 10 or more for a body covered with $CO_2$ or $CH_4$, which have much higher erosion yields than $H_2O$ (*19*). Under high-speed solar wind stream conditions, ion sputtering and sublimation can produce comparable water ice loss rates in a comet as close as at ~ 5 AU (*61*).

The growth, alteration, and erosion of grains in the interstellar medium are of great interest in astrophysics, as are the possible relations between processes on grains and the multitude of molecular cloud complexes seen throughout the galaxy (*62*). The possible alteration of the surface layers of "pristine" comets is also a topic of considerable importance (*19*). In view of recent results on molecule formation in the irradiation of ice mixtures (*12, 63*) (Fig. 4), perhaps the most important effect of ion irradiation of comets, minor planets such as Chiron, and interstellar grains is the alteration of the surface and subsurface (to the depths of penetration of the ions, a few tens of micrometers). Alterations in the surface composition would affect the nature of the spectra of a comet as it approached perihelion. Although such charged-particle irradiation experiments are just beginning, the initial results suggest that complex molecules can be formed on interstellar grain surfaces—molecules that are extremely difficult to form in gas-phase reactions. Ultraviolet irradiation forms such molecules (*64*) but the relative importances of ultraviolet- and ion-induced molecular formation is not known. In addition, the mechanisms of removal of such newly formed molecules from the grain surfaces require further study.

In summary, laboratory experiments to date have provided initial physical data needed for the investigation of a wide range of astrophysical problems involving ices in space. Applications to astrophysics will become even more quantitative as information on the velocity and species distributions of the ejected particles become available.

**References and Notes**


1. J. S. Lebofsky, *Icarus* **25**, 205 (1975).
2. C. B. Pilcher, S. T. Ridgway, T. B. McCord, *Science* **178**, 1087 (1972); L. A. Lebofsky, *Nature (London)* **269**, 785 (1977).
3. A. L. Broadfoot *et al.*, *Science* **204**, 979 (1979).
4. B. A. Smith *et al.*, *ibid.* **212**, 163 (1981).
5. F. L. Whipple, in *Comets, Asteroids and Meteorites*, D. H. Delsemme, Ed. (Univ. of Toledo Press, Toledo, Ohio, 1977), p. 25; *Astrophys. J.* **11**, 375 (1950).
6. K. C. Herr and G. C. Pimentel, *Science* **166**, 496 (1969); H. H. Kieffer, S. C. Chase, Jr., E. D. Miner, F. D. Palluconi, G. Münch, G. Neugebauer, T. Z. Martin, *ibid.* **193**, 780 (1976).
7. D. P. Cruikshank, C. B. Pilcher, D. Morrison, *ibid.*, **194**, 835 (1976); L. A. Lebofsky, G. H. Rieke, M. Lebofsky, *Icarus* **37**, 554 (1979); D. P. Cruikshank and P. M. Silvaggio, *ibid.* **41**, 96 (1980); B. T. Soifer, G. Neugebauer, K. Matthews, *Astron. J.* **85**, 166 (1980).
8. J. L. Bertaux and M. J. S. Belton, *Nature (London)* **282**, 813 (1979); W. D. Smythe, R. M. Nelson, D. B. Nash, *ibid.* **280**, 766 (1979); F. P. Fanale, R. H. Brown, D. P. Cruikshank, R. N. Clark, *ibid.*, p. 761; R. M. Nelson, A. L. Lane, D. L. Matson, F. P. Fanale, D. B. Nash, T. V. Johnson, *Science* **210**, 784 (1980).
9. A. H. Delsemme and D. C. Miller, *Planet. Space Sci.* **19**, 1229 (1971); A. H. Delsemme and A. Wagner, *ibid.* **18**, 709 (1970).
10. W. L. Brown, L. J. Lanzerotti, J. M. Poate, W. M. Augustyniak, *Phys. Rev. Lett.* **40**, 1027 (1978).
11. W. L. Brown, W. M. Augustyniak, E. Brody, L. J. Lanzerotti, A. L. Ramirez, R. Evatt, R. E. Johnson, *Nucl. Instrum. Methods* **170**, 321 (1980).
12. V. Pirronello, W. L. Brown, L. J. Lanzerotti, K. E. Marcantonio, E. Simmons, *Astrophys. J.*, in press.
13. P. Sigmund, *Phys. Rev.* **184**, 383 (1969).
14. P. D. Townsend, J. C. Kelly, N. E. W. Hartley, *Ion-Implantation, Sputtering and Their Applications* (Academic Press, New York, 1976); R. Behrisch, Ed., *Sputtering by Particle Bombardment* (Springer, Berlin, 1981).
15. W. L. Brown, W. M. Augustyniak, L. J. Lanzerotti, R. E. Johnson, R. Evatt, *Phys. Rev. Lett.* **45**, 1632 (1980).
16. B. H. Cooper, thesis, California Institute of Technology (1982); L. E. Seiberling, C. K. Meins, B. H. Cooper, J. E. Griffith, M. H. Mendenhall, T. A. Tombrello, *Nucl. Instrum. Methods* **198**, 17 (1982).
17. W. L. Brown *et al.*, *Nucl. Instrum. Methods* **198**, 1 (1982).
18. J. Bottiger, J. A. Davies, J. L'Ecuyer, H. K. Haugen, N. Matsunami, R. Ollerhead, in *Proceedings of a Conference on Ion Beam Modification of Materials, Budapest, 1978*, J. Gyulai, J. Lohner, E. Pasztor, Eds. (Central Research Institute for Physics, Budapest, 1979), p. 1521.
19. R. E. Johnson, L. J. Lanzerotti, W. L. Brown, W. M. Augustyniak, C. Musil, *Astron. Astrophys.*, in press.
20. L. J. Lanzerotti, W. L. Brown, W. M. Augustyniak, R. E. Johnson, T. P. Armstrong, *Astrophys. J.*, in press; P. K. Haff, C. C. Watson, Y. L. Yung, *J. Geophys. Res.* **86**, 6933 (1981).
21. F. Besenbacher, J. Bottiger, O. Graversen, J. L. Hansen, H. Sorensen, *Nucl. Instrum. Methods* **191**, 221 (1982).
22. R. Ollerhead, J. Bottiger, J. A. Davis, J. L'Ecuyer, H. J. Haugen, M. Matsunami, *Radiat. Effects* **49**, 203 (1980).
23. V. Pirronello, G. Strazzulla, G. Foti, E. Rimini, *Astron. Astrophys.* **96**, 267 (1980).
24. P. Borgesen and H. Sorensen, in preparation.
25. J. P. Biersack and E. Santer, *Nucl. Instrum. Methods* **132**, 229 (1976); M. Szymonski, H. Overeignder, A. E. de Vries, *Suf. Sci.* **90**, 274 (1979).
26. L. E. Seiberling, J. E. Griffith, T. A. Tombrello, *Radiat. Effects* **51**, 201 (1980).
27. Q. Yuanxun, J. E. Griffith, T. A. Tombrello, in preparation.
28. R. E. Johnson and W. L. Brown, *Nucl. Instrum. Methods* **198**, 103 (1982).
29. E. J. Hart and R. L. Platzman, in *Mechanisms in Radiation Biology*, M. Errera and A. Fonssberg, Eds. (Academic Press, New York, 1961), vol. 1, p. 93; J. E. Johnson and G. C. Moulton, *J. Chem. Phys.* **69**, 3108 (1978); J. A. Ghormley and A. C. Stewart, *J. Am. Chem. Soc.* **78**, 2934 (1956); J. J. Weiss, in *Physics of Ice*, N. Riehl, B. Bullemer, H. Englehartd, Eds. (Plenum, New York, 1969), p. 195.
30. R. E. Johnson and M. Inokuti, *Nucl. Instrum. Methods*, in press.
31. See for example, J. B. Hasted, *Physics of Atomic Collision* (American Elsevier, New York, ed. 2, 1972).
32. P. K. Haff, *Appl. Phys. Lett.* **29**, 473 (1976); J. O. Stiegler and T. S. Noggle, *J. Appl. Phys.* **33**, 1894 (1962).
33. G. H. Vineyard, *Radiat. Effects* **29**, 245 (1976); R. E. Johnson and R. Evatt. *ibid.* **52**, 187 (1980).
34. R. H. Ritchie and C. Claussen, *Nucl. Instrum. Methods* **198**, 133 (1982).
35. R. L. Fleischer, P. B. Price, R. M. Walker, *Nuclear Tracks in Solids, Principles and Applications* (Univ. of California Press, Berkeley, 1975).
36. M. W. Thompson, *Philos. Mag.* **18**, 377 (1968).
37. W. H. Ip, *J. Geophys. Res.* **86**, 1596 (1981).
38. T. W. Hill, A. J. Dessler, F. P. Fanale, *Planet. Space Sci.* **27**, 419 (1979).
39. L. J. Lanzerotti, W. L. Brown, J. M. Poate, W. M. Augustyniak, *Geophys. Res. Lett.* **5**, 155 (1978).
40. R. E. Johnson, L. J. Lanzerotti, W. L. Brown, T. P. Armstrong, *Science* **212**, 1027 (1981).
41. T. V. Johnson, *Annu. Rev. Earth Planet. Sci.* **6**, 93 (1978).
42. D. L. Matson, T. V. Johnson, F. P. Fanale, *Astrophys. J.* **192**, L43 (1974).
43. E. Sieveka and R. E. Johnson, *Icarus*, in press.
44. L. J. Lanzerotti, W. L. Brown, R. E. Johnson, *J. Geophys. Res.* **86**, 3449 (1981).
45. L. J. Lanzerotti, C. G. Maclennan, T. P. Armstrong, S. M. Krimigis, R. P. Lepping, N. F. Ness, *ibid.*, p. 8491.
46. R. N. Clark, *Icarus* **44**, 388 (1980).
47. P. K. Haff, C. C. Watson, T. A. Tombrello, *Proc. Lunar Planet Sci.* **100**, 1685 (1979); C. C. Watson, *ibid.* **128**, 1569 (1981).
48. R. E. Johnson, L. J. Lanzerotti, W. L. Brown, *Nucl. Instrum. Methods* **198**, 147 (1982).
49. U. Fink and H. P. Larsen, *Icarus* **24**, 411 (1975).
50. H. S. Bridge *et al.*, *Science* **204**, 987 (1979); J. W. Belcher, C. K. Goertz, H. S. Bridge, *Geophys. Res. Lett.* **7**, 17 (1980).
51. S. M. Krimigis *et al.*, *Science* **212**, 225 (1981).
52. A. F. Cheng, L. J. Lanzerotti, V. Pirronello, *J. Geophys. Res.* **87**, 4567 (1982).
53. L. Frank, B. Burek, K. Ackerson, J. Wolfe, J. M. Mihalov, *ibid.* **85**, 5995 (1980).
54. H. Weiser, R. C. Vitz, H. W. Moos, *Science* **197**, 755 (1977).
55. R. W. Carlson, *Nature (London)* **283**, 481 (1980).
56. A. F. Cheng and L. J. Lanzerotti, *J. Geophys. Res.* **83**, 2597 (1978).
57. L. J. Lanzerotti, W. L. Brown, J. M. Poate, W. M. Augustyniak, *Nature (London)* **272**, 431 (1978).
58. L. J. Lanzerotti and C. G. Maclennan, *J. Geophys. Res.* **78**, 3935 (1973).
59. H. Patashnick and G. Rupprecht, *Astrophys. J.* **197**, L79 (1975); *Icarus* **30**, 402 (1977).
60. T. Mukai and G. Schwehm, *Astron. Astrophys.* **95**, 373 (1981).
61. S. Wyckoff, in *Comets*, L. L. Wilkening, Ed. (Univ. of Arizona Press, Tucson, 1982).
62. M. A. Gordon and L. E. Snyder, Eds., *Molecules in the Galactic Environment* (Wiley-Interscience, New York, 1973); W. D. Watson, *Accounts Chem. Res.* **10**, 221 (1977); B. Zuckerman, *Nature (London)* **268**, 491 (1977); L. Spitzer, *Physical Processes in the Interstellar Medium* (Wiley, New York, 1978).
63. M. Moore and B. Donn, *Astrophys. J.*, in press.
64. J. M. Greenberg, *Astron. Space Sci.* **39**, 9 (1975).


65. A portion of the work at the University of Virginia was supported by NASA grant NAGW-186 and NSF grant AST-79-12690. One of us (R.E.J.) thanks U. Fano and A. Turkevitch for their hospitality while on leave at the University of Chicago.